

## Quantum spin chains with multiple dynamics

Xiao Chen,<sup>1</sup> Eduardo Fradkin,<sup>2</sup> and William Witczak-Krempa<sup>3</sup>

<sup>1</sup>*Kavli Institute for Theoretical Physics, University of California at Santa Barbara, California 93106, USA*

<sup>2</sup>*Department of Physics and Institute for Condensed Matter Theory, University of Illinois at Urbana-Champaign, 1110 West Green Street, Urbana, Illinois 61801-3080, USA*

<sup>3</sup>*Département de Physique, Université de Montréal, Montréal (Québec), Canada H3C 3J7*

(Received 23 June 2017; published 6 November 2017)

Many-body systems with multiple emergent time scales arise in various contexts, including classical critical systems, correlated quantum materials, and ultracold atoms. We investigate such nontrivial quantum dynamics in a different setting: a spin-1 bilinear-biquadratic chain. It has a solvable entangled ground state, but a gapless excitation spectrum that is poorly understood. By using large-scale density matrix renormalization group simulations, we find that the lowest excitations have a dynamical exponent  $z$  that varies from 2 to 3.2 as we vary a coupling in the Hamiltonian. We find an additional gapless mode with a continuously varying exponent  $2 \leq z < 2.7$ , which establishes the presence of multiple dynamics. In order to explain these striking properties, we construct a continuum wave function for the ground state, which correctly describes the correlations and entanglement properties. We also give a continuum parent Hamiltonian, but show that additional ingredients are needed to capture the excitations of the chain. By using an exact mapping to the *nonequilibrium* dynamics of a classical spin chain, we find that the large dynamical exponent is due to subdiffusive spin motion. Finally, we discuss the connections to other spin chains and to a family of quantum critical models in two dimensions.

DOI: [10.1103/PhysRevB.96.180402](https://doi.org/10.1103/PhysRevB.96.180402)

It is common for many-body quantum systems to possess multiple time scales that determine the low-energy dynamics. In a gapless system, the dynamics will be characterized by the dispersion relation of the excited states (quasiparticles need not exist),  $E = Ak^z$ , where  $k$  is the wave vector of the mode and  $z$  the dynamical exponent. Different modes can have different  $z$  exponents. For instance, a metal near a quantum critical point can have different dispersions for the electrons and the various order parameter fluctuations [1–6]. However, this phenomenon has been far less studied in other types of systems. Many studies have examined simpler systems, such as models described by relativistic conformal field theories (CFTs) having  $z = 1$ , which enjoy additional symmetries that constrain the dynamics [3,7,8].

In this Rapid Communication, we reveal multiple dynamical exponents in a different setting: a strongly correlated one-dimensional (1D) spin system. Further, these exponents will be shown to vary continuously as a function of a coupling in the Hamiltonian. The spin-1 quantum spin chain in question is a generalization of the so-called Motzkin Hamiltonian introduced by Bravyi *et al.* [9]. Its ground state can be determined exactly but not its excitation spectrum. With the help of large-scale density matrix renormalization group (DMRG) simulations, we discover low-lying excitations with different dynamical exponents. In order to gain insight in the low-lying spectrum, we determine a continuum version of the ground state, and find a parent Hamiltonian. The latter possesses an excitation spectrum that is distinct from the spin chain but can provide useful insight into the construction of the full low-energy field theory. This illustrates how a given ground state can have starkly different excitations, and offers some guidance in the construction of the true low-energy description of the chain. Owing to the Rokhsar-Kivelson [10] (RK) structure of the spin Hamiltonian, we are able to connect the problem of determining the excitation spectrum to studying the *nonequilibrium* dynamics of the corresponding classical

1D chain [11]. This sheds light on the subdiffusive nature ( $z > 2$ ) of the excitations observed with DMRG. Finally, we provide connections to a family of two-dimensional quantum critical systems that have conformally invariant wave functions [12,13].

*Critical quantum spin chain.* The Hamiltonian describes  $N$   $S = 1$  spins interacting via a nearest-neighbor exchange,

$$H_{\text{bulk}} = \sum_{i=1}^{N-1} |D\rangle_{i,i+1} \langle D| + |U\rangle_{i,i+1} \langle U| + c|V\rangle_{i,i+1} \langle V|, \quad (1)$$

where  $|D\rangle\sqrt{2} = |0d\rangle - |d0\rangle$ ,  $|U\rangle\sqrt{2} = |0u\rangle - |u0\rangle$ ,  $|V\rangle\sqrt{2} = |00\rangle - |ud\rangle$ ;  $c \geq 0$  is a free parameter. Here,  $u, d, 0$  label the  $S^z$  eigenstates. In terms of the spin operators  $S^{x,y,z}$ , Eq. (1) takes the form of an anisotropic bilinear-biquadratic Hamiltonian  $\sum_i (A_{ab} S_i^a S_{i+1}^b + B_{abcd} S_i^a S_{i+1}^b S_{i+1}^c S_{i+1}^d)$ ; we give the coefficients  $A, B$  in the Supplemental Material [14]. We will work with open chains with an additional boundary term,

$$H = H_{\text{bulk}} + \frac{1}{2} S_1^z (S_1^z - 1) + \frac{1}{2} S_N^z (S_N^z + 1). \quad (2)$$

$H$  has a global  $U(1)$  symmetry generated by  $S_{\text{tot}}^z = \sum_i S_i^z$  [15]. When  $c = 1$ ,  $H$  reduces to the so-called Motzkin Hamiltonian [9]. In that case, the ground state is the equal weight superposition of all states corresponding to Motzkin paths. For  $N = 3$ ,

$$|\mathcal{M}_3\rangle = \frac{1}{\sqrt{4}} (|---\rangle + |-\wedge\rangle + |\wedge-\rangle + |\vee-\rangle) \quad (3)$$

with the notation  $u = \swarrow$ ,  $d = \searrow$ ,  $0 = -$ . This allows for the height representation [9,15–17] shown in (3) and in Fig. 1: The height variable  $\phi_i$  is pinned to zero at both ends,  $\phi_0 = \phi_N = 0$ , while for  $i \geq 1$  we have  $S_i^z = \phi_i - \phi_{i-1}$ . In this language, a Motzkin path has  $\phi_i \geq 0$  while being pinned to zero at the extremities. By virtue of being an equal weight superposition, the Motzkin ground state  $|\mathcal{M}_N\rangle$  is annihilated by all three projectors in Eq. (1). It is thus a ground state when

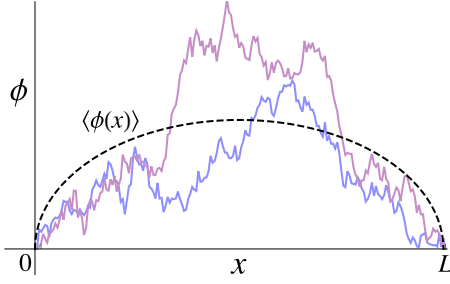


FIG. 1. Representation of two Motzkin paths via the height variable  $\phi$ . Each path can be interpreted as a Brownian excursion. The dashed line is the average of  $\phi$  in the ground state (4). The spin  $\langle S^z \rangle = \langle \partial_x \phi \rangle$  tends to zero deep in the bulk.

$c \geq 0$ . At  $c = 1$ , it was shown to be the unique ground state as a consequence of the boundary term, a fact which remains true as long as  $c > 0$  [9]. At the special point  $c = 0$ , other states belong to the ground-state manifold such as the all-zero product state.

*Ground state in the continuum.* In the continuum limit where  $x$  spans distances much larger than the lattice spacing, the ground-state wave function of the Motzkin Hamiltonian (2) takes the simple form

$$\Psi_0[\phi(x)] = \frac{1}{\sqrt{Z}} e^{-\frac{\kappa}{2} \int_0^L dx (\partial_x \phi)^2} \prod_x \theta[\phi(x)], \quad (4)$$

which is defined in terms of the (coarse-grained) height field  $\phi$  introduced above. This is reminiscent of the wave function of the quantum Lifshitz model in two dimensions (2D) [12,18], with the distinction that  $\phi$  here is noncompact. We discuss further connections between these models below. To match the boundary conditions of the lattice wave function, we impose the Dirichlet condition  $\phi(0) = \phi(L) = 0$  for a chain of length  $L$ . In this language, the spin field is given in the continuum by  $S^z = d\phi/dx$ ;  $\kappa$  is a parameter whose value will be fixed later and  $\theta(\phi)$  is the Heaviside function that enforces  $\phi$  to be non-negative. This constraint is necessary to obtain the Motzkin state [see Eq. (3)]. The normalization factor  $Z$  takes the form of a (0+1)-dimensional partition function,

$$Z = \int_{\phi(0)=\phi(L)=0} \mathcal{D}\phi(x) e^{-\kappa \int_0^L dx (\partial_x \phi)^2} \prod_x \theta[\phi(x)]. \quad (5)$$

The exponential term in the wave function (4), which determines the probability of a path  $\phi(x)$ , can be understood by mapping the problem to a random walk [9]. Let us momentarily go back to the lattice, which means that we need to consider discrete Brownian motion in 1D restricted to the *non-negative* integers  $\phi_i \geq 0$ . Taking the horizontal axis of the path  $i$  as the time direction, the random walk can be illustrated as follows. The walker takes a step chosen out of the three options: (1) Move up by one, (2) move down by one, or (3) stay at the same place. The walk is subject to the constraint  $\phi_i \geq 0$ , and it must start/end at the same point,  $\phi = 0$ , but is otherwise random. This process is called a Brownian excursion, and is illustrated in Fig. 1. Any valid path constructed out of a succession of such steps has the same probability, whose value is given by the Motzkin wave function squared  $P[\phi_i] = |\langle \phi_i | \mathcal{M}_N \rangle|^2$ .  $P$  thus equals the inverse of the total number of Motzkin paths.

Taking the long-time limit, the random walk is described by a Langevin equation for the continuum field  $\phi(x) \geq 0$ . Statistical physics [19] then tells us that the probability of a given path is given by the amplitude squared  $|\Psi_0[\phi(x)]|^2$  of our wave function (4). For the Motzkin-type random walk, the variance at a typical step is  $\sigma^2 = \frac{1}{3}[1^2 + 0^2 + (-1)^2] = 2/3$ . This determines the diffusion constant in the long-time limit,  $1/(4\kappa) = \sigma^2/2 = 1/3$ , i.e.,  $\kappa = 3/4$ . Equipped with our parameter-free wave function, we can compute properties of the ground state in the continuum limit. By comparing these properties with that for the discrete ground state, we can show that Eq. (4) and the ground state for Eq. (2) are exactly the same in the thermodynamical limit. For instance, the expectation value of the spin is  $\langle S^z(x) \rangle = \langle \partial_x \phi \rangle = (L - 2x)/\sqrt{\pi\kappa L(L - x)x}$ , which changes sign going from the left to the right end (see Fig. 1). The nonzero expectation value arises due to the boundary conditions. Indeed, deep in the bulk,  $\langle S^z(\frac{L}{2} + a) \rangle \propto a/L^{3/2}$  rapidly vanishes as  $L \rightarrow \infty$  at fixed  $a$ . This matches the calculation using the lattice wave function [9,15,20].

The Motzkin ground state is highly entangled in the sense that the Rényi entanglement entropy (EE) has a logarithmic scaling with subsystem size [9,15]. By considering the subregion  $A$  to be the interval  $[0, L_A]$ , we find, using (4),

$$S_n = \frac{1}{2} \ln \left( \frac{L_A(L - L_A)}{\epsilon L} \right) + b(n), \quad (6)$$

where the logarithm's prefactor is independent of the Rényi index  $n$  and of  $\kappa$ ;  $\epsilon$  is a short-distance cutoff. The constant  $b(n)$  depends on  $n, \kappa$ , and when we fix  $\kappa = 3/4$  we find an exact agreement with the lattice calculation [9,15]. The calculation of Eq. (6) is greatly simplified by the special form of the wave function Eq. (4), allowing us to adapt the methods of Ref. [21], described in the Supplemental Material [14]. Although in the limit  $L_A \ll L$ , the EE scales as  $\frac{1}{2} \ln L_A$ , the complete form of the EE is distinct from what is found in CFTs, and implies that the long-distance limit of the chain is not described by a CFT [9]. If we take region  $A$  to be an interval located deep inside the bulk, we find  $S_n = \frac{1}{2} \ln \frac{L_A}{\epsilon}$ .

The Motzkin wave function shows other clear differences from the ground state of a CFT, and is in fact less entangled. This can be seen by studying the mutual information for two disjoint intervals  $A, B$ , which was not studied before. The mutual information is defined as  $I(A, B) = S(A) + S(B) - S(A \cup B)$ . It measures the quantum correlations between  $A$  and  $B$ , giving an upper bound for two-point correlation functions of local observables [22]. In the wave function (4), for two disjoint intervals deep inside the bulk, we find  $I(A, B) = 0 + O(L_A L_B / L^2)$  [14]. This is consistent with the result for the spin two-point function,  $\langle S^z(x_1) S^z(x_2) \rangle = 0$  if  $x_1 \neq x_2$  in the Motzkin wave function [15], which can be readily derived using our continuum wave function [23]. The vanishing of  $I(A, B)$  can be understood by using the above mapping between the wave function (4) and the random walk problem. Deep inside the bulk, we can ignore the boundary conditions and remove the constraint  $\phi > 0$  due to the exponentially small probability for  $\phi$  being near zero in (4). In this regime the random walk reduces to regular Brownian motion, instead of the constrained Brownian excursion. Therefore, the probability for a walker moving a distance  $\delta\phi$  in "time"  $\delta x$  is independent

of the history. There are essentially no correlations between the two disjoint intervals and we expect that the mutual information between them in the quantum state vanishes. This stands in contrast with CFTs, for which the mutual information between two well-separated small intervals with distance  $r$  scales as  $1/r^\Delta$ , with  $\Delta$  determined by the scaling dimension of the primary operators [24].

The fact that the EE of a single interval diverges logarithmically but the mutual information between two intervals vanishes, suggests that nonlocal degrees of freedom are responsible for the entanglement measured via the EE. These escape the more “local” two-interval measures.

*A field theory with the Motzkin ground state.* We now take a step further and construct one quantum field theory whose ground state is (4), and has  $z \neq 1$ . The Hamiltonian of the field theory reads

$$H_{\text{orb}} = \int dx \left( \frac{1}{2} \Pi^2 + \frac{\kappa^2}{2} (\partial_x^2 \phi)^2 + V(\phi) \right). \quad (7)$$

$\Pi$  is the canonical conjugate to the height operator  $\phi$ .  $V(\phi)$  is the potential that enforces the constraint  $\phi \geq 0$ :  $V(\phi < 0) = \infty$  and is zero otherwise. Thus, the target space of  $\phi$  is the positive half line, i.e., the orbifold obtained by modding the real line by the transformation  $\phi \rightarrow -\phi$ . To show that (4) is the ground state of  $H_{\text{orb}}$ , we can rewrite the latter as  $H_{\text{orb}} = \int_x [Q^\dagger(x)Q(x) + V(\phi)]$ , where we have subtracted an infinite ground-state energy and defined the annihilation operator [12,18]  $Q(x) = \frac{1}{\sqrt{2}}(\frac{\delta}{\delta\phi} - \kappa \partial_x^2 \phi)$ . The ground state of Eq.(7) is annihilated by  $Q$ . This defines a functional equation that is satisfied by Eq. (4),  $Q\Psi_0[\phi] = 0$ .

Since  $\Pi = \partial_t \phi$ , we see that Eq. (7) is invariant under the spacetime dilation  $x \rightarrow \lambda x$  and  $t \rightarrow \lambda^2 t$  (with an appropriate field rescaling), implying that this Hamiltonian has a dynamical exponent  $z = 2$  and is thus not a CFT, in agreement with the EE results above. Now,  $H_{\text{orb}}$  and the continuum limit of the Motzkin Hamiltonian share the same ground state, but do they have the same low-energy excitations? To answer this question, we now investigate the excited states of Motzkin Hamiltonian Eq. (2). Because the problem is not readily amenable to analytical calculations, we turn to DMRG simulations.

*DMRG and dynamical exponents.* At  $c = 1$ , the many-body gap was shown to scale as  $1/N^z$ , with the analytical bound  $z \geq 2$  [16,25], suggesting that our above field theory is a viable candidate to describe the Motzkin Hamiltonian. However, exact diagonalization (ED) [9] on small systems yielded  $z = 2.91$ , while previous DMRG calculations [20] yielded  $z = 2.7 \pm 0.1$ . As we shall see, the former result suffers from strong finite size effects, while the latter does not correspond to the true lowest excited state. In order to understand the spectrum, we have performed large-scale DMRG calculations using the ITensor library, which we benchmarked using ED for short chains [14]. The results for  $z$  as a function of  $c$  are shown in Fig. 2. At  $c = 1$ , we find  $z = 3.16$  by using chains of length up to  $N = 100$ , an exponent substantially larger than the numerical results quoted above. The excitation associated with this dynamical exponent is twofold degenerate, with the two states having quantum numbers  $S_{\text{tot}}^z = \pm 1$ , respectively. Interestingly, we also found a singly degenerate excited state with higher energy in the  $S_{\text{tot}}^z = 0$  sector; it has a dynamical

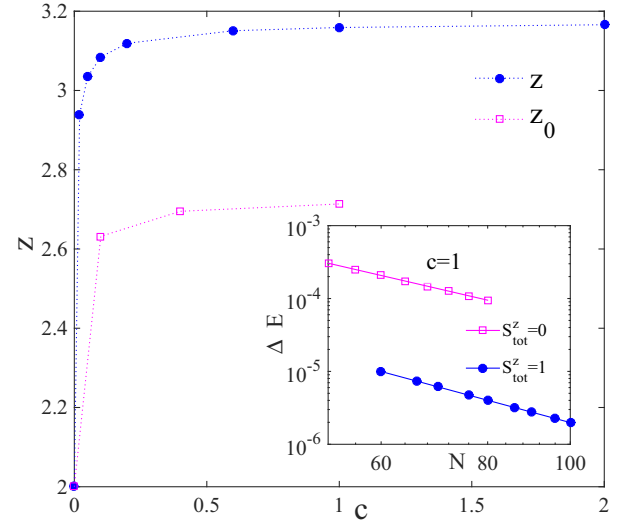


FIG. 2. DMRG data for the dynamical exponent of the generalized Motzkin Hamiltonian Eq. (2) vs the coupling  $c$ . The blue circles give  $z$  for the lowest excitation, which has  $S_{\text{tot}}^z = 1$ . The pink squares give  $z_0$  for the lowest excitation in the  $S_{\text{tot}}^z = 0$  sector. Inset: log-log plot of the energy gap vs system size  $N$  used to extract  $z$  via  $\Delta E \propto 1/N^z$ .

exponent  $z_0 = 2.71 < z$ . The proximity of  $z_0$  to the previous DMRG result [20] suggests that these authors worked in the  $S_{\text{tot}}^z = 0$  sector, thus missing the lowest excitations. We have also analyzed the excitations in the  $S_{\text{tot}}^z = 2$  sector and have found that they have the same dynamical exponent as in the  $S_{\text{tot}}^z = 1$  sector [14].

As we tune  $c$  away from 1, the ground state is still annihilated by all the local interaction terms, as is the case in (2) [9]. We find that  $H$  remains gapless but that the dynamical exponent  $z$  varies continuously with  $c$ . Figure 2 shows that  $z$  decreases monotonically as  $c$  decreases, and  $z > 2$  except when  $c = 0$ . Our DMRG results thus rule out the field theory above as the correct low-energy description of  $H$  for  $c > 0$ . Interestingly, it provides a concrete instance where different Hamiltonians, here the generalized Motzkin Hamiltonian Eq. (2) and  $H_{\text{orb}}$  Eq. (7), can have the same ground state but markedly distinct excitations. At the special point  $c = 0$ ,  $H$  has  $z = 2$  by virtue to a mapping to the ferromagnetic Heisenberg spin-1/2 chain [9]. In that case, the ground-state manifold becomes highly degenerate, growing exponentially with  $N$ , and contains the all-zero product state. We can construct an exact excited state in the form of a spin wave. Since we are interested in the thermodynamic limit, we can work with an infinitely long chain, in which case the excited state reads  $\sum_j e^{ikj} |u\rangle_j |0\rangle_{\text{rest}}$ , where  $k$  specifies the wave number of the mode. The wave has  $S_{\text{tot}}^z = 1$  and energy  $1 - \cos k$ , leading to  $z = 2$  at small  $k$ .

We now provide physical insight into the result  $z > 2$  observed when  $c > 0$ . Earlier we have seen how the ground-state properties of the generalized Motzkin Hamiltonian map to the classical Brownian motion of a particle. We can go further and study the *full spectrum* of the Hamiltonian of Eq. (2) by examining the nonequilibrium dynamics of a *classical* 1D spin chain. Indeed, the RK form of  $H$  ensures that we can map

the quantum spin chain problem to the dynamics of classical chain governed by a Markovian master equation [11,26,27]. The nondiagonal elements of the rate matrix  $W$  are given by the matrix elements of  $H$  between spin configurations,  $W_{C,C'} = -(C|H|C')$ ; the diagonal elements of  $W$  follow from a detailed balance. The quantum dynamics of (2) thus maps to the critical slowing down of the corresponding classical model endowed with dynamics  $W$ .

Hohenberg and Halperin have classified the critical slowing down of classical critical models according to the symmetries of the low-energy modes [28]. For instance, the Glauber dynamics of an Ising chain belongs to model A because single spin flip (nonconserving) processes are allowed. In this case, the motion of a domain wall is described by the diffusion equation yielding a dynamical exponent  $z = 2$  [28]. In contrast, the generalized Motzkin Hamiltonian (2) maps to classical dynamics described by the model B universality class since the spin flipping processes preserve  $S_{\text{tot}}^z$ . The conservation law constrains the spin flips and can thus slow down the dynamics, leading to a larger  $z$  [13,29]. For instance, the spin-conserving Kawasaki dynamics of an Ising chain show  $z \approx 3$  in a certain temperature range [29,30]. In Fig. 2, we also observe such subdiffusive behavior with  $z \approx 3$ . To understand such behavior, it is useful to analyze the physics near  $c = 0$ , where we have shown above that  $z = 2$  results from the diffusive motion of an up spin in a sea of 0's. As we turn on  $c > 0$ , the  $|V\rangle\langle V|$  projector in Eq. (1) generates more  $ud$  pairs, which slow down the motion of the up spin. Indeed, imagine we create an  $ud$  pair next to an  $u$  spin,  $0uud0$ . Using the projectors in Eq. (1), it takes three moves to translate the leftmost  $u$  one site to the right, as opposed to one move in the absence of the  $ud$  pair. This argument suggests that the dynamics slow down as  $c$  increases, in agreement with our DMRG results in Fig. 2, but does not explain the specific change of  $z$  with  $c$ , nor the presence of excitations with different dynamical exponents. One can get quantitative results for  $z$  by performing a Monte Carlo sampling of the nonequilibrium classical spin chain, as we mention below. Finally, it would be desirable to obtain a field theory description for the full spectrum. We expect that marginal operators play a key role in explaining the change of the dynamical exponents with  $c$ .

*Summary and outlook.* We have studied the intricate dynamics of a  $S = 1$  quantum spin chain, Eq. (2). Our

DMRG simulations have revealed that the gapless system has a dynamical exponent  $z$  that changes as a function of a coupling  $c$  in the Hamiltonian (Fig. 2). Interestingly, similar behavior was observed in quantum critical lattice models in two spatial dimensions [13], where the Hamiltonian also takes a RK form. These authors used the mapping to the nonequilibrium dynamics of a classical model described above in order to determine  $z$  via classical Monte Carlo simulations; dynamics with a varying  $z > 2$  were also observed. It would be interesting to analyze these 2D Hamiltonians further to see if an additional excitation with a smaller  $z$  appears, just as in our case. The Monte Carlo methods could also be applied in our case to reach bigger system sizes. A further connection is that the 2D ground states studied in Ref. [13] have an emergent *spatial* conformal symmetry [12,13,18], a feature that also arises in the generalized Motzkin model, although in a more subtle way [23]. We should also note that systems with modes that scale with different dynamic critical exponents have been found in theories of the quantum nematic transition in 2D metals [4–6]. Finally, although we focused on spin 1, the physics we discussed applies to other quantum spin chains, such as spin-1/2 ones, even without an RK structure [23]. We thus see the emergence of a unified picture for a broad class of quantum critical systems with nontrivial dynamics. An important missing element in both 1D and 2D is a field theory description, although our present analysis might help guide the search. This program will also shed light on the nonequilibrium dynamics of classical systems via the exact map of Henley discussed above [11].

We thank A. Ludwig, R. Movassagh, S. Sachdev, M. Stoudenmire, and X. Yu for useful discussions. X.C. was supported by a postdoctoral fellowship from the Gordon and Betty Moore Foundation, under the EPIQS initiative, Grant No. GBMF4304, at the Kavli Institute for Theoretical Physics. This work was supported in part by the U.S. National Science Foundation through Grant No. DMR-1408713 at the University of Illinois (E.F.). W.W.K. was funded by a Discovery Grant from NSERC, and by a Canada Research Chair. The DMRG simulations were performed using the ITENSOR package (version 2). We acknowledge support from the Center for Scientific Computing from the CNSI, MRL, an NSF MRSEC (DMR-1121053).

- 
- [1] J. A. Hertz, Quantum critical phenomena, *Phys. Rev. B* **14**, 1165 (1976).
  - [2] A. J. Millis, Effect of a nonzero temperature on quantum critical points in itinerant fermion systems, *Phys. Rev. B* **48**, 7183 (1993).
  - [3] S. Sachdev, *Quantum Phase Transitions*, 2nd ed. (Cambridge University Press, Cambridge, UK, 2011).
  - [4] V. Oganesyan, S. A. Kivelson, and E. Fradkin, Quantum theory of a nematic Fermi fluid, *Phys. Rev. B* **64**, 195109 (2001).
  - [5] T. Meng, A. Rosch, and M. Garst, Quantum criticality with multiple dynamics, *Phys. Rev. B* **86**, 125107 (2012).
  - [6] S. Lederer, Y. Schattner, E. Berg, and S. A. Kivelson, Superconductivity and non-Fermi liquid behavior near a nematic quantum critical point, *Proc. Natl. Acad. Sci. USA* **114**, 4905 (2017).
  - [7] P. Di Francesco, P. Mathieu, and D. Sénéchal, *Conformal Field Theory* (Springer, New York, 1996).
  - [8] A. Lucas, S. Gazit, D. Podolsky, and W. Witczak-Krempa, Dynamical Response near Quantum Critical Points, *Phys. Rev. Lett.* **118**, 056601 (2017).
  - [9] S. Bravyi, L. Caha, R. Movassagh, D. Nagaj, and P. W. Shor, Criticality without Frustration for Quantum Spin-1 Chains, *Phys. Rev. Lett.* **109**, 207202 (2012).
  - [10] D. S. Rokhsar and S. A. Kivelson, Superconductivity and the Quantum Hard-Core Dimer Gas, *Phys. Rev. Lett.* **61**, 2376 (1988).
  - [11] C. L. Henley, From classical to quantum dynamics at Rokhsar Kivelson points, *J. Phys.: Condens. Matter* **16**, S891 (2004).

- [12] E. Ardonne, P. Fendley, and E. Fradkin, Topological order and conformal quantum critical points, *Ann. Phys.* **310**, 493 (2004).
- [13] S. V. Isakov, P. Fendley, A. W. W. Ludwig, S. Trebst, and M. Troyer, Dynamics at and near conformal quantum critical points, *Phys. Rev. B* **83**, 125114 (2011).
- [14] See Supplemental Material at <http://link.aps.org/supplemental/10.1103/PhysRevB.96.180402> for results that support the conclusions of the main text (4 pages, including 3 figures).
- [15] R. Movassagh, Entanglement and correlation functions of the quantum Motzkin spin-chain, *J. Math. Phys.* **58**, 031901 (2017).
- [16] R. Movassagh and P. W. Shor, Supercritical entanglement in local systems: Counterexample to the area law for quantum matter, *Proc. Natl. Acad. Sci. USA* **113**, 13278 (2016).
- [17] Z. Zhang, A. Ahmadain, and I. Klich, Novel quantum phase transition from bounded to extensive entanglement, *PNAS Proc. Natl. Acad. Sci. USA* **114**, 5142 (2017).
- [18] E. Fradkin, *Field Theories of Condensed Matter Physics* (Cambridge University Press, Cambridge, UK, 2013).
- [19] S. N. Majumdar, Brownian functionals in physics and computer science, *Curr. Sci.* **89**, 2076 (2005).
- [20] L. Dell'Anna, O. Salberger, L. Barbiero, A. Trombettoni, and V. E. Korepin, Violation of cluster decomposition and absence of light cones in local integer and half-integer spin chains, *Phys. Rev. B* **94**, 155140 (2016).
- [21] E. Fradkin and J. E. Moore, Entanglement Entropy of 2D Conformal Quantum Critical Points: Hearing the Shape of a Quantum Drum, *Phys. Rev. Lett.* **97**, 050404 (2006).
- [22] M. M. Wolf, F. Verstraete, M. B. Hastings, and J. I. Cirac, Area Laws in Quantum Systems: Mutual Information and Correlations, *Phys. Rev. Lett.* **100**, 070502 (2008).
- [23] X. Chen, E. Fradkin, and W. Witczak-Krempa, Gapless quantum spin chains: Multiple dynamics and conformal wave functions, *J. Phys. A: Math. Theor.* **50**, 464002 (2017).
- [24] P. Calabrese, J. Cardy, and E. Tonni, Entanglement entropy of two disjoint intervals in conformal field theory II, *J. Stat. Mech.: Theory Exp.* (2011) P01021.
- [25] D. Gosset and E. Mozgunov, Local gap threshold for frustration-free spin systems, *J. Math. Phys.* **57**, 091901 (2016).
- [26] R. Moessner, S. L. Sondhi, and E. Fradkin, Short-ranged resonating valence bond physics, quantum dimer models, and Ising gauge theories, *Phys. Rev. B* **65**, 024504 (2001).
- [27] C. Castelnovo, C. Chamon, C. Mudry, and P. Pujol, From quantum mechanics to classical statistical physics: Generalized Rokhsar-Kivelson Hamiltonians and the stochastic matrix form decomposition, *Ann. Phys.* **318**, 316 (2005).
- [28] P. C. Hohenberg and B. I. Halperin, Theory of dynamic critical phenomena, *Rev. Mod. Phys.* **49**, 435 (1977).
- [29] M. D. Grynberg, Revisiting Kawasaki dynamics in one dimension, *Phys. Rev. E* **82**, 051121 (2010).
- [30] R. Cordery, S. Sarker, and J. Tobochnik, Physics of the dynamical critical exponent in one dimension, *Phys. Rev. B* **24**, 5402 (1981).